Article:
Waheed, QMK, Wu, C and Williams, PT (2016) Pyrolysis/reforming of rice husks with a Ni–dolomite catalyst: Influence of process conditions on syngas and hydrogen yield. Journal of the Energy Institute, 89 (4). pp. 657-667. ISSN: 1743-9671

https://doi.org/10.1016/j.joei.2015.05.006

Pyrolysis-reforming of rice husks with a Ni-dolomite catalyst: Influence of process conditions on syngas and hydrogen yield

Qari M. K. Waheed, Chunfei Wu and Paul T. Williams*

Energy Research Institute, University of Leeds, Leeds, LS2 9JT, UK

*(Tel: #44 1133432504; Email: p.t.williams@leeds.ac.uk)

ABSTRACT

The influence of process conditions on the production of syngas and H_2 from biomass in the form of rice husks was investigated using a two-stage pyrolysis-catalytic reforming reactor. The parameters investigated were, reforming temperature, steam flow rate and biomass particle size and the catalyst used was a 10 wt.% Ni-dolomite catalyst. Biomass was pyrolysed in the first stage, and the product volatiles were reformed in the second stage in the presence of steam and the Ni-dolomite catalyst. Increase in catalyst temperature from 850 °C to 1050 °C marginally improved total syngas yield. However, H_2 yield was increased from 20.03 mmoles g^{-1} at 850 °C to 30.62 mmoles g^{-1} at 1050 °C and H_2 concentration in the product gas increased from 53.95 vol.% to 65.18 vol.%. Raising the steam flow rate increased the H_2 yield and H_2 gas concentration. A significant increase in H_2**:**CO ratio along with a decrease in CO**:**CO_2 ratio suggested a change in the equilibrium of the water gas shift reaction towards H_2 formation with increased steam flow rate. The influence of particle size on H_2 yield was small showing an increase in H_2 production when the particle size was reduced from 2.8 – 3.3 to 0.2 – 0.5 mm.

Keywords: Pyrolysis; Reforming; Biomass; Rice husk; Hydrogen

1. Introduction

Fossil fuels such as coal, oil and gas are a finite resource and their use in energy systems is adding large quantities of greenhouse gases into the atmosphere every year leading to concerns related to climate change [1,2]. In order to maintain a sustainable supply of energy together with a reduction in greenhouse gases emissions, it is essential to find alternative and cleaner sources of energy. Hydrogen has been suggested as such a future energy source which is currently largely produced from fossil fuels via natural gas steam reforming or coal gasification [3]. However, hydrogen production from fossil fuels is considered unsustainable and alternative, more carbon-neutral sources for hydrogen production are under consideration [3]. Hydrogen may be produced from biomass via gasification/reforming processes [4-7]. The process of biomass gasification/reforming is still developing and there are challenges related to the upgrading and cleaning of the product synthesis gas. There is therefore interest in optimizing the gasification/reforming process operating parameters so that little or no cleaning equipment is required to upgrade the product syngas. High temperature thermal processing of biomass has been undertaken to reduce the tar content of the flue gases. Septien et al. [8] undertook the fast pyrolysis of woody biomass in a drop tube furnace at temperatures of 1000, 1200 and 1400 °C. Increasing pyrolysis temperature produced increased yield of gas and also increased H_2. There was a consequent decrease in tar content and $C_1 - C_6$ hydrocarbons. Zhang et al [9] investigated the pyrolysis, steam gasification and partial oxidation of biomass in a drop-tube furnace over a wide temperature range (600 − 1400 °C). They reported that H_2 production increased with increasing temperature for all the thermal processes investigated. They suggested that hydrogen is produced from pyrolysis of biomass at higher temperatures due to dehydrogenation of cellulose, hemicelluloses and lignin and decomposition of the pyrolysis

product tars and hydrocarbons. When steam was added to the process, the water gas shift reaction further enhanced H_2 production. Skolou et al [10] reported on the steam gasification of biomass in a fixed bed reactor at temperatures from 750 − 1050 °C to maximise H_2 production. Hydrogen production increased with increasing temperature, reaching values of more than 40 vol.% in the product syngas.

There has been recent research into using two-stage pyrolysis-catalytic reforming processes to reduce tar contents and increase the gas yield, particularly for H_2 production. In the two stage process, biomass is pyrolysed in the first stage and then the product effluent gases, volatiles, and tar are gasified in the second stage already at higher temperature (T > 800 °C). Addition of a gasifying agent such as steam along with a catalyst in the second stage has also shown a positive effect on biomass to gas conversion and H_2 yield [11-13]. Nickel based catalysts are typically used for H_2 production in the gasification/reforming process, due to their effective catalytic performance and the reported lower cost compared to, for example, noble metal catalysts [13, 14]. Cao et al [15] used a two-stage fixed bed reactor with a Ni/Al_2O_3 catalyst for the pyrolysis-catalytic steam reforming of biomass in the form of sewage sludge. They produced a H_2 – rich syngas with a H_2 content of 68 vol.%. The effect of the addition of the nickel catalyst was to double the production of H_2 compared to steam only pyrolysis-reforming. Wu et al [13] also used a two-stage fixed bed reactor with an Ni/MCM-41 catalyst with different nickel metal loadings for the pyrolysis-catalytic steam reforming of wood. Maximum gas yield was found with the higher nickel content at 62.8 wt.%, and maximum H_2 concentration was 50.6 vol.%. The work was extended to a continuous two-stage pyrolysis–catalytic steam reforming reactor using waste wood and various nickel-based catalysts [12]. Maximum syngas yield of 54.0 wt.% was produced with a NiO/SiO_2 catalyst and maximum H_2 production of 44.4 vol.% was obtained with a NiO/Al_2O_3 catalyst.

The influence of process parameters on the biomass/gasification of biomass has been investigated by various researchers [4,5,8,10,16,17] and process operating parameters such as gasification/reforming temperature, steam flow rate and biomass particle size have been investigated. For example, Luo et al. [4,5] investigated the influence of gasification/reforming temperature, steam flow rate and particle size in a fixed bed reactor. They reported that smaller particle size produced higher gas and H_2 yield and higher temperatures (600 – 900 °C) also significantly increased gas and H_2 yield. In addition, the introduction of steam leads to reforming of the product tars and consequently, higher gas yield and carbon conversion. Franco et al. [16] researched a range of process parameters and different biomass types for the fluidised bed steam gasification process, H_2 yield increased as the temperature of the fluidised bed reactor was raised from 700 to 900 °C. Blanco et al. [18] investigated the influence of catalyst temperature for the two-stage catalytic steam reforming of biomass in the form of refuse derived fuel. Increasing the second stage temperature in the absence of catalyst resulted in an increase in gas and H_2 yield, and when nickel based catalyst were introduced the gas and H_2 yields were markedly increased with increasing catalyst temperature.

In our previous work, we used a two-stage pyrolysis-catalytic reforming reactor system to compare the H_2 yield from rice husks, sugarcane bagasse and wheat straw in the presence of dolomite and Ni-dolomite catalysts [6]. The second stage catalytic reforming was carried out at 950 °C and the results showed that H_2 production was increased in the presence of the Ni-dolomite. There is interest in using low cost dolomite-based catalysts and higher temperatures to maximise the production of H_2. In this study, we investigate the influence of various process parameters in relation to the production of syngas and H_2 for the pyrolysis-catalytic steam reforming of rice husks in a two-stage reactor system with a 10 wt.% Ni-

dolomite catalyst. The different process conditions investigated were catalyst temperature (850 - 1050 °C), steam flow rate, and particle size.

2. Materials and methods

2.1. Biomass

Rice (*Oryza sativa*) husk biomass was sourced from Pakistan. The rice husk biomass was ground and sieved to obtain different particle size ranges of 0.2 – 0.5 mm, 0.5 – 1.0 mm, 1.4 - 2.8 mm and 2.8 – 3.3 mm. These samples were kept in air tight containers to ensure the consistent composition until final usage.

2.2. Catalyst

A 10 wt.% Ni-dolomite was used in this study and was synthesised in the laboratory using a wet impregnation method [7]. A known quantity of $Ni(NO_3)_2.6H_2O$ was dissolved in 25 ml of deionized water, 10 g of dolomite was then dissolved in the solution and heated to 105 °C with constant stirring. The catalyst was dried overnight at 105 °C and then calcined at 900 °C for 3 hours in an air atmosphere. The catalyst was later ground and sieved to achieve a final particle size between 0.050 - 0.212 mm.

2.3. Materials characterization

A Stanton Redcroft 1000 thermogravimetric analyser (TGA) operating at atmospheric pressure was used to carry out the proximate analysis of the rice husk biomass sample. The

rice husk contained 63.71 wt.% volatiles and 12.98 wt.% fixed carbon and ash and moisture contents in the rice husk were found to be 17.21 wt.% and 6.1 wt.% respectively. A Thermoquest CE Flash EA 2000 series instrument was used for C, H, N and S analysis of the rice husk and the results showed that 39.82 wt.% of carbon, 5.4 wt.% of hydrogen and 1.27 wt.% of nitrogen were present in the rice husk. No sulphur content was detected and oxygen content calculated by difference was 53.51 wt%.

The freshly prepared and used catalysts were characterised using a range of techniques. The BET (Brunauer, Emmett and Teller) surface area, pore volume, and pore size distribution of the fresh catalyst was measured using a Nova-2200e surface area and pore size analyser from Quantachrome instruments USA. The average pore size and BJH pore volume of the fresh 10 wt.% Ni-dolomite catalyst were found to be 2.21 nm and 0.0308 cm^3 g^{-1} respectively. Adsorption and desorption curves were obtained by increasing the relative pressure from 0 to 1 at 77 K using liquid nitrogen. A Nonlocal density function theory (NLDFT) equilibrium model was used to calculate the pore volume and pore size distribution.

The deposition of carbon on the used catalysts after reaction was investigated by temperature programmed oxidation (TPO) using a Stanton Redcroft 1000 thermogravimetric analyser. The used catalyst after reaction was heated in an air atmosphere, from ambient temperature to 800 °C at 15 °C min^{-1} heating rate, with a dwell time of 10 min. The amount of carbon deposited on the catalyst was calculated using Equation (1).

$$w = \frac{(w_1 - w_2)}{w_1} \times 100 \text{ (wt\%)} \qquad (1)$$

Where w is the amount of deposited carbon on catalyst in wt.%. w_1 is the initial catalyst weight after moisture loss and w_2 is the final catalyst weight after oxidation.

A field emission gun scanning electron microscope (FEGSEM) LEO 1530 equipped with 80 mm X-Max SDD detector was used to analyse the microscopic structure of fresh and reacted catalysts. Each specimen was coated with 10 - 15 nm platinum layer. High resolution electron microscopy was carried out under vacuum conditions at 2.5 - 3 mm working distance with a supply voltage of 3 KV.

2.4. Experimental reactor

Pyrolysis of biomass samples (4g) and catalytic steam reforming of effluent pyrolysis volatiles was carried out in a two stage fixed bed reactor system, 60 cm in length with 2.5 cm inner diameter and constructed of Inconel (Fig. 1). The reactor system consisted of two stages, a pyrolysis stage and catalytic reforming stage, each separately heated by electrical furnaces. Nitrogen was used as purge gas. The first stage produces pyrolysis gases which are then passed directly to the second stage containing the catalyst and the pyrolysis volatiles are gasified/reformed in the presence of steam and the catalyst. During this study, the second stage catalytic reactor was heated to 950 °C except when the influence of catalytic reforming temperature was studied (850, 900, 950, 1000, and 1050 °C). The Ni-dolomite catalyst (2 g) was placed on a perforated mesh placed in the reforming reactor. Once the second stage reactor reached the required temperature, heating up of the pyrolysis stage began along with the steam injection in the second stage. During all experiments, the pyrolysis stage was heated at 20 °C min^{-1} to 950 °C. Steam was introduced into the reforming reactor via water injected from a syringe pump which was immediately converted into steam at high temperature and swept through the reactor by the nitrogen carrier gas. The steam to biomass ratio was 1.37 for all experiments since steam was introduced at 6 ml h^{-1} for 55 minutes. When the parameter of steam flow rate was studied, the water flow rate was 2, 4, 6, and 10 ml h^{-1} representing steam to biomass ratios of 0.46, 0.91, 1.37 and 2.28 respectively. The

catalyst temperature was maintained at 950 °C. Product exit gases and excess steam was condensed in a series of condensers. The non-condensable gases were collected using a Tedlar™ gas sample bag and were analysed off-line using gas chromatography. The particle size of rice husk chosen for this study was in the range of 1.4 - 2.8 mm except when the influence of rice husk particle size was studied (0.2 – 0.5, 0.5 – 1.0, 1.4 – 2.8, and 2.8 – 3.3 mm). Repeatability experiments were performed on the reactor system to ensure the reliability and suitability of the system for the current research work.

2.5. Gas analysis

Two different gas chromatographs (GC's) were used to analyse the gas samples collected in the gas sample bag. The gases were analysed for hydrocarbons (C_1-C_4) using a Varian CP-3380 gas chromatograph with a column packed with an 80-100 mesh HayeSep with a flame ionization detector (GC/FID) and using nitrogen as carrier gas. Permanent gases (H_2, CO, N_2, O_2, CO_2) were analysed using a second Varian CP-3380 gas chromatograph comprised of two columns with two thermal conductivity detectors (GC/TCD). One column packed with a 60-80 mesh molecular sieve, was used to separate H_2, CO, N; and the other column packed with 80-100 mesh HayeSep was used to analyse CO_2; the carrier gas used was argon.

3. Results and discussion

3.1. Influence of catalytic reforming temperature

3.1.1. Product yield

Temperature is one of the most influential parameters affecting not only the gas yield but also the gas composition during pyrolysis and catalytic reforming [19]. In this study, the

temperature of the pyrolysis stage was increased from ambient to 950 °C at 20 °C min^{-1} while the temperature of the catalytic reforming stage was kept constant at either, 850, 900, 950, 1000, or 1050 °C. The particle size used was 1.4 – 2.8 m.m. and the steam flow rate was 6 ml h^{-1} (steam to biomass ratio 1.37). The results are shown in Table 1. The results show that with the increase in temperature, gas yield in relation to biomass increased from 60.49 wt.% at 850 °C to 67.66 wt.% at 1000 °C and decreased slightly to 61.84 wt.% at 1050 °C. Wang et al. [20] reported an increase in gas yield from 0.98 Nm^3 kg^{-1} to 1.33 Nm^3 kg^{-1} of feedstock with the increase in temperature from 750 to 900 °C during the two-stage catalytic gasification/reforming of pig compost using a Ni-modified dolomite catalyst. The increase in the gas yield with the increase in catalytic reforming temperature was primarily due to the thermal cracking of volatiles, liquids and steam reforming of hydrocarbons [21]. At higher temperature, the endothermic Boudouard reaction and water gas reaction also contributed towards the higher gas yield. Decarboxylation, depolymerization and thermal cracking reactions are also favoured with the increase in temperature [22]. The slight decrease in gas yield at the highest studied temperature of 1050 °C was most likely due to the series of complex repolymerization and condensation reactions favourable at temperature above 1000 °C [8,23]. These condensation and repolymerization reactions lead to the formation of soot as a significant amount of soot was observed in the system during the 1050 °C experiment.

One of the advantages of high temperature catalytic steam catalytic reforming used in this study was the enhanced gas and H_2 yield with lower tar contents. Devi et al. [24] reported that as compared to olivine, the use of dolomite at higher temperature was more effective leading to a substantial decrease in all categories of tar compounds. Skoulou et al. [10] found a significant decrease in tar from 124.07 g Nm^{-3} at 750 °C to 25.26 g Nm^{-3} at 1050 °C during the high temperature steam gasification/reforming of olive kernel. Although the concentration of tar reduced with the rise in temperature, it was noticed that at 1050 °C tar was mainly

composed of light aromatic hydrocarbons with a fraction of polycyclic aromatic hydrocarbons and heterocyclic compounds as compared to heavy tars found at 750 °C.

3.1.2. Influence of temperature on gas composition and hydrogen production

Table 1 shows that H_2 yield in the gaseous mixture increased with the rise in temperature, H_2 yield was enhanced from 20.03 mmoles g^{-1} of rice husk at 850 °C to 30.62 mmoles g^{-1} at 1050 °C. Fig. 2 shows the gas concentration in the product gases for H_2 CO, CO_2, CH_4, and $C_2 – C_4$ hydrocarbons. The H_2 concentration was increased from 53.95 vol.% at 850 °C to 65.18 vol.% at 1050 °C. Results presented here are in agreement with the findings of González et al. [25] who reported 27.63 moles of H_2 per kilogram of olive cake during the two-stage dolomite catalytic steam gasification/reforming at 900 °C. They also reported around 52 vol.% of H_2 from the two-stage gasification of olive cake at 900 °C. Skoulou et al. [10] reported an increase in H_2 gas concentration from less than 10 vol.% at 750 °C to ~42 vol.% at 1050 °C during steam gasification/reforming of olive kernel in a fixed bed gasifier.

The increase in H_2 concentration with the increase in the catalyst reforming temperature is linked to the higher temperature which favours endothermic reactions (e.g. water gas reaction and Boudouard reaction) [19]. As shown in Table 1, with the increase in temperature, CO**:**CO_2 ratio was increased from 1.08 to 1.57 indicating the effectiveness of the Boudouard reaction. Steam reforming and dry reforming of methane and other higher hydrocarbons also contribute towards the higher H_2 concentration. The increase in H_2**:**CO_2 ratio from 2.83 at 850 °C to 4.87 at 1050 °C showed the effectiveness of high temperature for dry reforming reactions. A decrease in CO_2 concentration from 19.06 vol.% at 850 °C to 13.38 vol.% at 1050 °C was most likely due to the Boudouard reaction and dry reforming reactions. Similarly H_2**:**CH_4 ratio was also enhanced from 8.68 at 850 °C to 186.23 at 1050

°C showing effective steam reforming reaction as CH_4 concentration was decreased from 6.22 vol.% at 850 °C to 0.35 vol.% at 1050 °C. Thermal cracking of hydrocarbons and tar components also lead to enhanced H_2 yield at higher catalytic reforming temperatures [26]. Only 0.12 vol.% lighter hydrocarbons (C_2-C_4) were detected at 850 °C and no C_2-C_4 hydrocarbons were detected at 900 °C or above (Fig. 2). A similar decrease in concentrations of CH_4 and lighter hydrocarbons during the steam gasification/reforming of wood biomass was reported by Franco et al. [16].

Fig. 2 also shows that the concentration of CO was almost constant at ~ 21 vol.% as the CO produced from different endothermic reactions such as water gas, Boudouard reaction and steam methane reforming was consumed by the water gas shift reaction to produce H_2 because the H_2**:**CO ratio was slightly increased from 2.61 at 850 °C to 3.09 at 1050 °C. However the extent of equilibrium of each reaction depends on many factors as various competing parallel reactions would be taking place simultaneously in the second stage catalytic reactor.

3.1.3. Characterization of reacted catalysts

The surface area of the fresh 10 wt.% Ni-dolomite catalyst calcined at 900 °C was 5.56 $m^2\ g^{-1}$ and after reaction was reduced to 4.33 $m^2\ g^{-1}$ at 850 °C catalyst temperature, 2.80 $m^2\ g^{-1}$ at 1000 °C and to 1.94 $m^2\ g^{-1}$ at 1050 °C catalyst temperature. Therefore, a gradual reduction in surface area of the reacted catalyst with the increase in temperature was observed. This decrease in surface area was most likely due to sintering of Ni particles on the dolomite support which is indicated in the scanning electron micrographs shown in Fig. 3 where agglomeration and loss of surface structure is seen with increased temperature. Sehested et al. [27,28] reported a decrease in surface area from 122 $m^2\ g^{-1}$ at 500 °C to 84.8 $m^2\ g^{-1}$ at 825 °C during their investigations on sintering of 9.5 wt.% Ni-Al_2O_3 catalyst.

Sintering is a complex process depending on various factors such as temperature, time, atmosphere and nickel-support interaction. It has been reported [29] that the higher temperature and higher partial pressure of steam tend to promote sintering while increase in partial pressure of hydrogen showed an inhibitory effect on the sintering of nickel [27]. It has been suggested that the increase in the rate of sintering at higher temperature is due to the change of sintering mechanism from particle migration and coalescence (PMC) to Ostwald ripening (OR) [30]. Hansen et al. [31] suggested three phases of sintering during their investigation of nanoparticles; rapid loss of catalytic activity during phase I, slowdown of sintering during phase II, and a stable catalytic activity after particle growth and support restructuring during phase III.

Temperature programmed oxidation using thermogravimetric analysis (TGA-TPO) of the used catalysts was carried out and the results are shown in Fig. 4. The negligible carbon deposition at 1000 °C, suggests that the two-stage pyrolysis/catalytic reforming at this high temperature was effective against coking of the catalyst. As shown in Fig. 4, except for the catalyst temperature of 1050 °C, a gradual decrease in carbon deposition was observed with the increase in temperature; from 2.46 wt.% at 850 °C to 1.17 wt.% at 950 °C. No carbon deposits were detected for the catalyst used at 1000 °C. This decrease in carbon deposition was most likely due to the enhanced endothermic Boudouard and water gas reactions at elevated temperature converting the carbon into gaseous species such as CO and CO_2. The TGA-TPO and DTG-TPO results shown in Fig. 4, indicate that the highest carbon deposits of 3.89 wt.% were found on the catalyst at 1050 °C. It has been suggested that above 1000 °C, the tertiary tars (polyaromatic hydrocarbons), acted as a precursor for the formation of soot [32]. These polycyclic aromatic hydrocarbon molecules grow into larger aromatic complexes until they reach a critical mass, forming soot particles [8].

As shown in Fig. 4, all the catalysts showed two weight loss peaks; a first peak at a temperature at ~430 °C and a second higher temperature peak at ~640 °C. It has been suggested that the first peak of weight loss may be attributed to the oxidation of amorphous carbons while the second peak was due to the presence of filamentous carbon [33,34].

3.2. Influence of steam flow rate

3.2.1. Product yield

The influence of steam flow rate on gas yield and H_2 production was investigated via the pyrolysis of 4 grams of rice husks while the steam flow rate was varied from 2, 4, 6 and 10 ml h^{-1}, representing steam to biomass ratios of 0.46, 0.91, 1.37 and 2.28 respectively. The particle size used was 1.4 – 2.8 m.m. and the N-dolomite catalyst temperature used was 950 °C. The results are shown in Table 2. From these results, it is evident that the gas yield in relation to biomass (corrected for no input water) slightly increased from 61.61 wt.% for 2 ml h^{-1} to 64.23 wt.% for 10 ml h^{-1} steam flow rate. Xiao et al. [35] also reported an increase in gas yield with the increase in stream to carbon ratio during the two-stage gasification/reforming of wood chips and pig compost in a fluidized bed reactor. A decrease in tar contents with the increase in steam to feedstock ratio was reported by Xiao et al [36]. Meng et al. [37] also reported a reduction in the concentration of all classes of tar with the increase in steam to carbon ratio.

Higher gas yield with the increase in steam flow rate was obtained because the higher steam flow rates promote steam reforming of tar and other hydrocarbons from the pyrolysis of the rice husk biomass leading to the higher gas yield [35,38]. The water gas reaction is also suggested to have played a role in enhancing the gas yield. Hu et al. [39] investigated the influence of steam to biomass ratio on gas yield from the two stage gasification/reforming of

apricot stones at 800 °C. They reported that the H_2 and potential H_2 production increased with an increase in the steam to biomass ratio from 0.4 - 0.8 however it decreased slightly with the increase in steam to biomass ratio from 0.8 - 1.2. González et al. [25] also reported an increase in gas yield with the increase in steam flow rate during the two-stage gasification/reforming of olive cake.

3.2.2. Influence of steam flow rate on gas composition and hydrogen production

The influence of steam flow rate on gas composition is shown in Fig. 5. The H_2 concentration in the product gas increased from 56.29 vol.% to 61.88 vol.% with the increase in steam flow rate from 2 ml h^{-1} to 10 ml h^{-1}. Similarly the H_2 yield shown in Table 2, increased from 22.31 mmoles g^{-1} of rice husk for 2 ml h^{-1} steam flow rate to 27.86 mmoles g^{-1} of rice husk for 10 ml h^{-1} steam flow rate. Similar trends were reported by Xiao et al [35,36]. This increase in H_2 yield was most likely due to the water gas reaction, the water gas shift reaction, methane steam reforming reaction and steam reforming of tar hydrocarbon components [40].

The concentration of CO decreased from 28.84 vol.% to 19.66 vol.% with the increase in steam flow rate from 2 ml h^{-1} to 10 ml h^{-1}, however, the concentration of CO_2 was enhanced slightly from 14.13 vol.% to 16.26 vol.%. This decrease in CO concentration along with the increase in CO_2 concentration was most likely due to the water gas shift reaction [25]. The water gas shift reaction is slightly exothermic and production of H_2 is not favoured at higher temperature. However, according to Le Chatelier's principle, the equilibrium can be shifted to favour hydrogen production by increasing the concentration of one of the reactants, in this case the steam flow rate. A significant increase in H_2**:**CO ratio from 1.95 at 2 ml h^{-1} to 3.15 at 10 ml h^{-1} along with a decrease in CO**:**CO_2 ratio from 2.04 to 1.21 suggests CO_2 and H_2 formation via the water gas shift reaction. Karmakar et al. [41] reported an increase in H_2

and CO_2 concentration along with a decrease in CO and CH_4 concentration when the steam to biomass ratio was varied from 0.6 to 1.70 during the steam catalytic reforming of rice husk at 750 °C. They reported that H_2 concentration was enhanced from 47.81 vol.% to 51.89 vol.% while CO concentration was reduced from 27.48 vol.% to 17.38 vol.%.

A slight increase in CH_4 concentration from 0.74 vol.% at 2 ml h^{-1} to 2.20 vol.% at 10 ml h^{-1} was found, most likely due to the methanation reaction [16,25]. A decrease in H_2**:**CH_4 ratio from 75.59 at 2 ml h^{-1} to 28.15 at 10 ml h^{-1} suggests CH_4 formation via methanation reaction. Due to the high temperature employed in this study, no other hydrocarbons were detected. Franco et al. [16] studied the influence of steam to biomass ratio on gas yield and gas composition from the gasification/reforming of soft wood and hard wood in a fluidized bed reactor at 800 °C. They reported an initial increase in H_2 concentration with the increase in steam to biomass ratio from 0.5 to 0.7. However further increase in steam to biomass ratio led to a slight decrease in H_2 concentration. It was suggested that at lower steam to biomass ratios, there was not enough steam available to react with the biomass and hence to attain equilibrium in the gas product while at higher steam to biomass ratios, it was speculated that the secondary water gas reaction might have resulted in the formation of H_2 and CO_2. A similar trend was also reported by Hu et al. [39] during the two stage gasification/reforming of apricot stones at 800 °C. They reported that the H_2 yield and H_2 potential increased for a steam to biomass ratio of 0.4 - 0.8 however it decreased slightly with the further increase in steam to biomass ratio from 0.8 - 1.2.

3.3. Influence of biomass particle size

3.3.1. Product yield

The influence of biomass particle size on product yield from the pyrolysis-catalytic steam reforming of rice husks was investigated and the results are shown in Table 3. The

Ni-dolomite catalyst temperature used was 950 °C and the steam flow rate was 6 ml h^{-1}. The gas yield in relation to biomass (corrected for no input water) only slightly increased from 63.83 wt.% for the largest particle size range (2.8 – 3.3 mm) to 66.24 wt.% for the smallest particle size range (0.2 – 0.5 mm). Similar findings have been reported in the literature [4,17,42,43] For example, Li et al. [43] reported an increase in gas yield from 2.16 to 2.41 m^3 kg^{-1} when the particle size was reduced from 5 mm to < 0.15 mm during two stage gasification (800 °C) and catalytic reforming (850 °C) of palm oil waste.

Luo et al. [4] suggested that higher gas yield was due to the improved mass and heat transfer which resulted from smaller particle diameter and larger surface area to volume ratio. This makes it easier for most volatiles to evolve, leaving behind very porous char particles. For porous char particles, gasification reactions take place throughout the particle instead of only at the surface; hence the rate of reaction is controlled by chemical kinetics instead of heat and mass transfer [4,44]. Babu et al. [45] mentioned that less time was required for the complete conversion of smaller particles. Furthermore, Luo et al. [4] noted that for different particle sizes, the difference in gas yield was more pronounced at lower temperature of 600 °C while gas yield tended to merge at the higher temperature of 900 °C. It was suggested that this convergence was due to the increase in effective thermal conductivity at higher temperatures.

3.3.2. Influence of particle size on gas composition and hydrogen production

The influence of rice husk particle size on gas composition is shown in Fig. 6. The results show that H_2 concentration in the product gas mixture was slightly improved from 59.45 vol.% for the largest particle size (2.8 – 3.3 mm) to 63.12 vol.% for the smallest particle size range (0.2 – 0.5 mm). The H_2 yield for the pyrolysis-catalytic steam reforming of rice husks shown in Table 3, also increased from 25.05 mmoles g^{-1} to 29.13 mmoles g^{1} as the

particle size was reduced. Luo et al. [4], Hernández et al. [17] and Rapagnà et al. [46] also reported an increase in H_2 concentration with the decrease in particle size. Luo et al. [4] suggested that the increase in H_2 concentration with the decrease in particle size was due to the enhanced gas phase reaction. Wei et al. [44] suggested that the smaller biomass particles pyrolysed sufficiently and more volatiles were released. In this study, the variation in biomass particle size showed only a small influence on H_2 production. This was most likely due to the higher temperatures employed in this study which resulted in effective heat transfer and lower internal heat conduction resistance of the biomass particles. In addition, the elemental and proximate analysis of the various size fractions may have been altered by the sieving process. For example, the high ash content of the rice husks may have differentially fractionated into different particle sizes, thereby consequently altering the organic content of each size fraction.

A reduction in CO concentration from 21.53 vol.% to 17.81 vol.% with the decrease in particle size from 2.8 – 3.3 mm to 0.2 – 0.5 mm (Fig. 6) suggests the formation of H_2 via the water gas shift reaction as indicated by an increase in H_2**:**CO ratio from 2.76 to 3.54 along with the decrease in CO**:**CO_2 ratio from 1.24 to 0.99 (Table 3). A slight reduction in CH_4 concentration (from 1.62 vol.% to 1.08 vol.%) was most likely due to the methane steam reforming reaction [42], as H_2**:**CH_4 ratio was increased from 36.75 to 58.39 with the decrease in particle size from 2.8 – 3.3 mm to 0.2 – 0.5 mm.

4. Conclusions

The influence of the process conditions; catalytic reforming temperature, steam flow rate and biomass particle size during the two-stage pyrolysis-catalytic reforming of rice husks

in a fixed-bed reactor system was performed with the aim to obtain high syngas and H_2 yield. It may be concluded that;

With the increase in catalytic reforming temperature from 850 °C to 1050 °C, H_2 yield was significantly increased from 20.03 to 30.62 mmoles H_2 per gram of rice husks. It was suggested that the higher gas yield was primarily due to the endothermic Boudouard reaction, water gas reaction and steam reforming reaction. Decarboxylation, depolymerization and thermal cracking reactions also played a major role in increasing H_2 concentration (from 53.95 to 65.18 vol.%) in the product gas.

Increase in steam flow rate from 2 ml h^{-1} (steam: biomass ratio 0.46) to 10 ml h^{-1} (steam: biomass ratio 2.28) showed a small but positive influence on gas yield (increased from 61.61 wt.% to 64.23 wt.%) as well as H_2 yield (increased from 22.31 to 27.86 mmoles g^{-1}). Hydrogen concentration in the product gas was improved from 56.29 vol.% to 61.88 vol.%. A significant increase in H_2**:**CO ratio from 1.95 at 2 ml h^{-1} to 3.15 at 10 ml h^{-1} along with a decrease in CO**:**CO_2 ratio from 2.04 to 1.21 suggests that the water gas reaction played a major role in CO_2 and H_2 formation.

With the decrease in particle size from 2.8 – 3.3 to 0.2 – 0.5 mm, H_2 yield was slightly increased from 25.05 to 29.13 mmoles H_2 per gram of rice husk. Gas yield was also marginally increased with the decrease in biomass particle size.

Acknowledgements

The financial support provided by the Government of Pakistan for one of us (Q. M.K.W.) is gratefully acknowledged.

References

[1]. International Energy Agency Key World Energy statistics. 2012, International Energy Agency, 9, rue de federation, 75739 Paris Cedex 15 - France. p. 82.

[2]. S. Shafiee, E. Topal, When will fossil fuel reserves be diminished? Energ. Policy 37 (2009) 181-189.

[3]. H. Balat, E. Kirat Hydrogen from biomass-present scenario and future prospects. Int. J. Hydrogen Energy 35 (2010) 7416-7426.

[4]. S. Luo, B. Xiao, X. Guo, Z. Hu, S. Liu, M. He. *Hydrogen-rich gas from catalytic steam gasification of biomass in a fixed bed reactor: Influence of particle size on gasification performance.* Int. J. Hydrogen Energ. 34 (2009) 1260-1264.

[5]. S. Luo, B. Xiao, Z. Hu, S. Liu, X. Guo, M He. *Hydrogen-rich gas from catalytic steam gasification of biomass in a fixed bed reactor: Influence of temperature and steam on gasification performance.* Int. J. Hydrogen Energ. 34 (2009) 2191-2194.

[6]. Q.M.K. Waheed, P.T. Williams, Hydrogen Production from High Temperature Pyrolysis/Steam Reforming of Waste Biomass: Rice Husk, Sugar Cane Bagasse, and Wheat Straw. Energ. Fuel. 27 (2013) 6695-6704.

[7]. C. Wu, P.T. Williams, Ni/CeO2/ZSM-5 catalysts for the production of hydrogen from the pyrolysis–gasification of polypropylene. Int. J. Hydrogen Energ. 34 (2009) 6242-6252.

[8]. S. Septien, S. Valin, C. Dupont, M. Peyrot, S. Salvador. Effect of particle size and temperature on woody biomass fast pyrolysis at high temperature (1000–1400°C). Fuel 97 (2012) 202-210.

[9]. Y. Zhang, S. Kajitani, M. Ashizawa, Y. Oki. Tar destruction and coke formation during rapid pyrolysis and gasification of biomass in a drop-tube furnace. Fuel 89 (2010) 302-309.

[10]. V. Skoulou, A. Swiderski, W. Yang, A. Zabaniotou. Process characteristics and products of olive kernel high temperature steam gasification (HTSG). Biores. Technol. 100 (2009) 2444-2451.

[11]. Z. Ma, S.P. Zhang, D.Y. Xie, Y.J. Yan. A novel integrated process for hydrogen production from biomass. Int. J. Hydrogen Energy 39 (2014) 1274-1279.

[12]. C.E. Efica, C. Wu, P.T. Williams. Syngas production from pyrolysis-catalytic steam reforming of waste biomass in a continuous screw kiln reactor. J. Anal. Appl. Pyrol. 95 (2012) 87-94.

[13]. C. Wu, P.T. Williams. Hydrogen production from biomass gasification with Ni/MCM-41 catalysts: Influence of Ni content. Appl. Cat. B Environ. 108 (2011) 6-13.

[14]. T. Kimura, T. Miyazawa, J. Nishikawa, S. Kado, K. Okumura, T. Miyao, S. Naito, K. Kunimori, K. Tomishige, Development of Ni catalysts for tar removal by steam gasification of biomass. Appl. Catal. B-Environ. 68 (2006) 160-170.

[15]. J.P. Cao, P. Shi, X.Y. Zhao, X.Y. Wei, T. Takarada. Catalytic reforming of volatiles and nitrogen compounds from sewage sludge pyrolysis to clean hydrogen and synthetic gas over a nickel catalyst. Fuel Proc. Technol. 123 (2014) 34-40.

[16]. C. Franco, F. Pinto, I. Gulyurtlu, I. Cabrita. The study of reactions influencing the biomass steam gasification process. Fuel 82 (2003) 835-842.

[17]. J.J. Hernández, G. Aranda-Almansa, A. Bula, Gasification of biomass wastes in an entrained flow gasifier: Effect of the particle size and the residence time. Fuel Proc. Technol. 91 (2010) 681-692.

[18] P.H. Blanco, C. Wu, J.A. Onwudili, P.T. Williams P.T., Characterisation of tar from the pyrolysis/gasification of refuse derived fuel: Influence of process parameters and catalysis. Energ. Fuel. 26 (2012) 2107-2115.

[19]. E.L. Taba, M.F. Irfan, W.A.M.W. Daud, M.H. Chakrabati. The effect of temperature on various parameters in coal, biomass and CO-gasification: A review. Renew. Sus. Energ. Rev. 16 (2012) 5584-5596.

[20]. J. Wang, B. Xiao, S. Liu, Z. Hu, P. He, D. Guo, M. Hu, F. Qi, S. Luo. Catalytic steam gasification of pig compost for hydrogen-rich gas production in a fixed bed reactor. Biores. Technol. 133 (2013) 127-133.

[21]. Q. Xie, S. Kong, Y. Liu, H. Zeng. Syngas production by two-stage method of biomass catalytic pyrolysis and gasification. Biores. Technol. 110 (2012) 603-609.

[22]. W. F. Fassinou, L. Van de Steene, S. Toure, G. Volle, P. Girad. Pyrolysis of Pinus pinaster in a two-stage gasifier: Influence of processing parameters and thermal cracking of tar. Fuel Proc. Technol. 90 (2009) 75-90.

[23]. K. Qin, W. Lin, P.A. Jensen, A.D. Jensen. High-temperature entrained flow gasification of biomass. Fuel 93 (2012) 589-600.

[24]. L. Devi, K.J. Ptasinki, F.J.J.G. Janssen, S.V.B. van Paasen, P.C.A. Bergman, J.H.A. Kiel. Catalytic decomposition of biomass tars: use of dolomite and untreated olivine. Renew. Energ. 30 (2005) 565-587.

[25]. J.F. González, S. Roman, G. Engo, J.M. Encinar, G. Martinez. Reduction of tars by dolomite cracking during two-stage gasification of olive cake. Biomass Bioenerg., 35 (2011) 4324-4330.

[26]. P. Lahijani, Z.A. Zainal. Gasification of palm empty fruit bunch in a bubbling fluidized bed: A performance and agglomeration study. Biores. Technol. 102 (2011) 2068-2076.

[27]. J. Sehested, J.A.P. Gelten, I.N. Remediakis, H. Bengard, J.K. Norskov. Sintering of nickel steam-reforming catalysts: effects of temperature and steam and hydrogen pressures. J. Catal. 223 (2004) 432-443.

[28]. J. Sehested. Sintering of nickel steam-reforming catalysts. J. Catal. 217 (2003) 417-426.

[29]. J. Sehested, J.A.P. Gelten, S. Helveg. Sintering of nickel catalysts: Effects of time, atmosphere, temperature, nickel-carrier interactions, and dopants. Appl. Catal. A Gen. 309 (2006) 237-246.

[30]. J. Sehested. Four challenges for nickel steam-reforming catalysts. Catal. Today 111 (2006) 103-110.

[31]. T.W. Hansen, A.T. De La Riva, R.R. Challa, A.K. Datye. Sintering of Catalytic Nanoparticles: Particle Migration or Ostwald Ripening? Acc. Chem. Res. 46 (2013) 1720-1730.

[32]. J.J. Hernández, R. Ballesteros, G. Aranda. *Characterisation of tars from biomass gasification: Effect of the operating conditions.* Energy, 50 (2013) 333-342.

[33]. S. Wang, G.Q Lu. *A Comprehensive Study on Carbon Dioxide Reforming of Methane over Ni/γ-Al2O3 Catalysts.* Ind. Eng. Chem. Res. 38 (1999) 2615-2625.

[34]. M.A. Goula, A.A. Lemonidou, A.M. Efstathiou, *Characterization of Carbonaceous Species Formed during Reforming of CH4with CO2over Ni/CaO–Al2O3Catalysts Studied by Various Transient Techniques.* J. Catal. 161 (1996) 626-640.

[35]. X. Xiao, X. Meng, D.D. Le, T. Takarada. Two-stage steam gasification of waste biomass in fluidized bed at low temperature: Parametric investigations and performance optimization. Biores. Technol. 102 (2011) 1975-1981.

[36]. X. Xiao, D.D. Le, K. Morishita, S. Zhang, L. Li, T. Takarada. Multi-stage biomass gasification in Internally Circulating Fluidized-bed Gasifier (ICFG): Test operation of animal-waste-derived biomass and parametric investigation at low temperature. Fuel Proc. Technol. 91 (2010) 895-902.

[37]. X. Meng, W. de Jong, N. Fu, A.H.M. Verkooijen. Biomass gasification in a 100 kWth steam-oxygen blown circulating fluidized bed gasifier: Effects of operational conditions on product gas distribution and tar formation. Biomass Bioenerg. 35 (2011) 2910-2924.

[38]. J. Srinakruang, K. Sato, T. Vitidsant, K. Fujimoto. Highly efficient sulfur and coking resistance catalysts for tar gasification with steam. Fuel 85 (2006) 2419-2426.

[39]. G. Hu, S. Xu, S. Li, C. Xiao, S. Liu. Steam gasification of apricot stones with olivine and dolomite as downstream catalysts. Fuel Proc. Technol. 87 (2006) 375-382.

[40]. X.T. Li, J.R. grace, C.J. Lim, A.P. Watkinson, H.P. Chen, J.R. Kim. Biomass gasification in a circulating fluidized bed. Biomass Bioenerg. 26 (2004) 171-193.

[41]. M.K. Karmakar, A.B. Datta, Generation of hydrogen rich gas through fluidized bed gasification of biomass. Biores. Technol. 102 (2011) 1907-1913.

[42]. Y. Wang, C.M. Kinoshita, Kinetic model of biomass gasification. Solar Energ. 51 (1993) 19-25.

[43]. J. Li, Y. Yan, X. Zhang, J. Liu, R. Yan. Hydrogen-rich gas production by steam gasification of palm oil wastes over supported tri-metallic catalyst. Int. J. Hydrogen Energ. 34 (2009) 9108-9115.

[44]. L. Wei, S. Xu, L. Zhang, H. Zhang, C. Liu, H. Zhu, S. Liu. Characteristics of fast pyrolysis of biomass in a free fall reactor. Fuel Proc. Technol. 87 (2006) 863-871.

[45]. B.V. Babu, A.S. Chaurasia, Modeling for pyrolysis of solid particle: kinetics and heat transfer effects. Energ. Convers. Manag. 44 (2003) 2251-2275.

[46]. S. Rapagnà, A. Latif, Steam gasification of almond shells in a fluidised bed reactor: the influence of temperature and particle size on product yield and distribution. Biomass Bioenerg. 12 (1997) 281-288.

Table 1. The influence of catalytic reforming temperature on pyrolysis-catalytic reforming of rice husk (particle size; 1.4 – 2.8 m.m. and steam to biomass ratio 1.37)

	Temperature (°C)				
	850 Ni-dolomite Catalyst	900 Ni-dolomite Catalyst	950 Ni-dolomite Catalyst	1000 Ni-dolomite Catalyst	1050 Ni-dolomite Catalyst
H_2 (mmoles g^{-1} rice husk)	20.03	21.47	25.44	29.02	30.62
H_2/CO	2.61	2.38	2.59	2.78	3.09
CO/CO_2	1.08	1.39	1.41	1.43	1.57
H_2/CO_2	2.83	3.29	3.64	3.96	4.87
H_2/CH_4	8.68	17.36	33.24	194.8	186.23
CH_4/CO	0.3	0.14	0.08	0.01	0.02
CH_4/CO_2	0.33	0.19	0.11	0.02	0.03
Mass balance (wt.%)					
Gas / (biomass + water)	23.29	24.83	26.30	27.99	26.62
Solid / (biomass + water)	12.13	12.96	13.02	13.34	13.56
Mass balance	98.75	96.02	96.65	95.62	92.93
Gas / (biomass)	60.49	60.33	63.64	67.66	61.84
Solid / (biomass)	31.5	31.5	31.5	32.25	31.5

Table 2. The influence of steam flow rate on pyrolysis /catalytic reforming of rice husk (particle size 1.4 – 2.8 m.m. and catalyst temperature 950 °C).

	Steam flow rate (ml h^{-1})			
	2	4	6	10
Steam: biomass ratio	0.46	0.91	1.37	2.28
H_2 (mmoles g^{-1} rice husk)	22.31	25.9	25.44	27.86
H_2/CO	1.95	2.21	2.59	3.15
CO/CO_2	2.04	2.1	1.41	1.21
H_2/CO_2	3.99	4.65	3.64	3.8
H_2/CH_4	75.59	37.51	33.24	28.15
CH_4/CO	0.03	0.06	0.08	0.11
CH_4/CO_2	0.05	0.12	0.11	0.14
Mass balance (wt.%)				
Gas / (biomass + water)	42.49	33.4	26.3	18.62
Solid / (biomass + water)	22.41	16.54	13.02	9.06
Mass balance	96.63	91.41	96.65	95.64
Gas / (biomass)	61.61	63.63	63.64	64.23
Solid / (biomass)	32.5	31.5	31.5	31.25

Table 3. The influence of particle size on pyrolysis-catalytic reforming of rice husk (catalyst temperature 950 °C and steam: biomass ratio 1.37).

	Particle size (mm)			
	0.2 – 0.5	0.5 - 1.0	1.4 – 2.8	2.8 – 3.3
H_2 (mmoles g^{-1} rice husk)	29.13	26.74	25.44	25.05
H_2/CO	3.54	2.7	2.59	2.76
CO/CO_2	0.99	1.41	1.41	1.24
H_2/CO_2	3.51	3.82	3.64	3.42
H_2/CH_4	58.39	44.22	33.24	36.75
CH_4/CO	0.06	0.06	0.08	0.08
CH_4/CO_2	0.06	0.09	0.11	0.09
Mass balance (wt.%)				
Gas / (biomass + water)	27.09	27.44	26.3	26.13
Solid / (biomass + water)	14.11	13.32	13.02	13
Mass balance	93.14	92.34	96.65	94.81
Gas / (biomass)	66.24	64.89	63.64	63.83
Solid / (biomass)	34.5	31.5	31.5	31.75

FIGURE CAPTIONS

Fig. 1. Schematic diagram of the two-stage fixed-bed high temperature reactor

Fig. 2. The influence of catalytic reforming temperature on gas composition during the pyrolysis-catalytic steam reforming of rice husk ((particle size; 1.4 – 2.8 m.m. and steam to biomass ratio 1.37).

Fig. 3. SEM images of fresh and reacted catalysts showing the influence of catalytic reforming temperature (a) fresh 10 wt.% Ni-dolomite , (b) reacted 10 wt.% Ni-dolomite at 850 °C, (c) reacted at 900 °C, (d) reacted at 950 °C, (e) reacted at 1000 °C and (f) reacted at 1050 °C

Fig. 4. TGA-TPO and DTG-TPO results showing the influence of catalytic reforming temperature on the amount of deposited carbon on reacted 10 wt.% Ni-dolomite catalyst

Fig. 5. The influence of steam flow rate on gas composition during the pyrolysis-catalytic reforming of rice husk (particle size 1.4 – 2.8 m.m. and catalyst temperature 950 °C).

Fig. 6. The influence of particle size on gas composition during the pyrolysis-gasification of rice husk (catalyst temperature 950 °C and steam: biomass ratio 1.37).

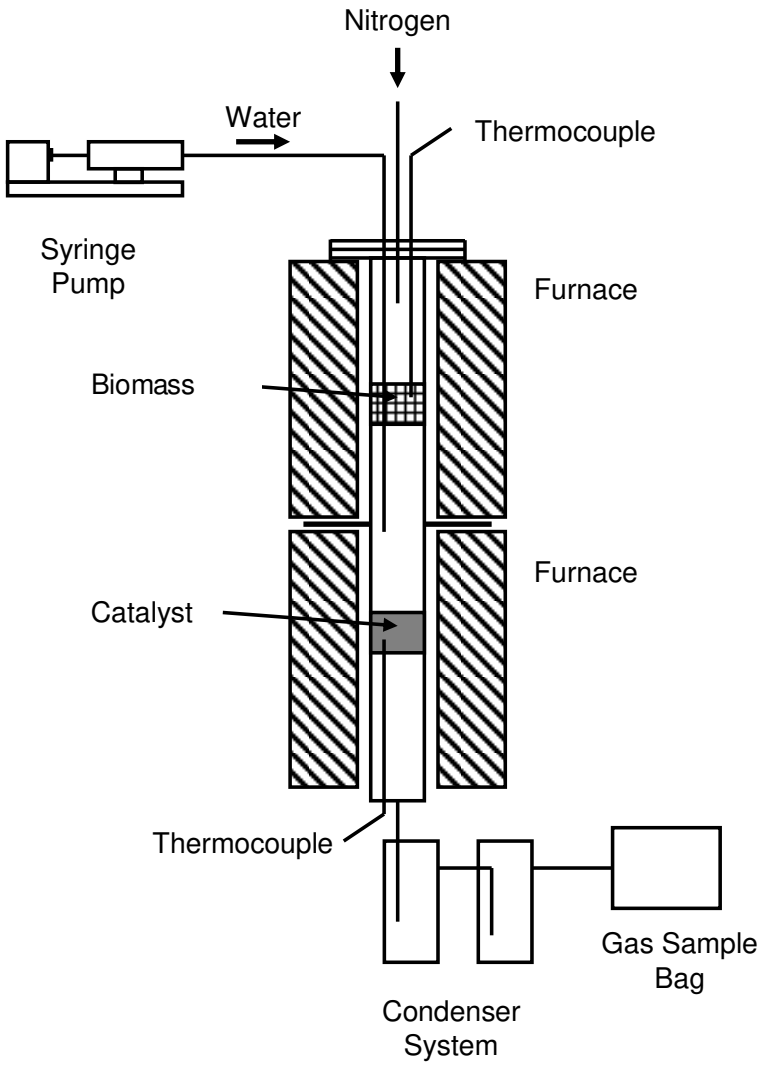

Fig. 1. Schematic diagram of the two-stage fixed-bed high temperature reactor

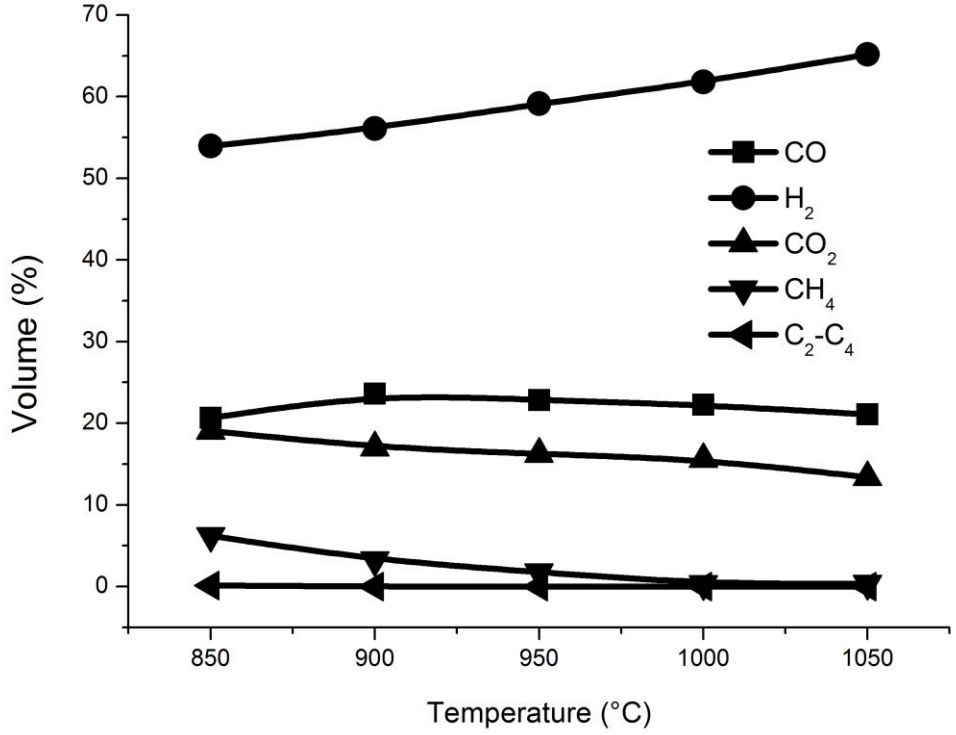

Fig. 2. The influence of catalytic reforming temperature on gas composition during the pyrolysis-catalytic steam reforming of rice husk (particle size; 1.4 – 2.8 m.m. and steam to biomass ratio 1.37).

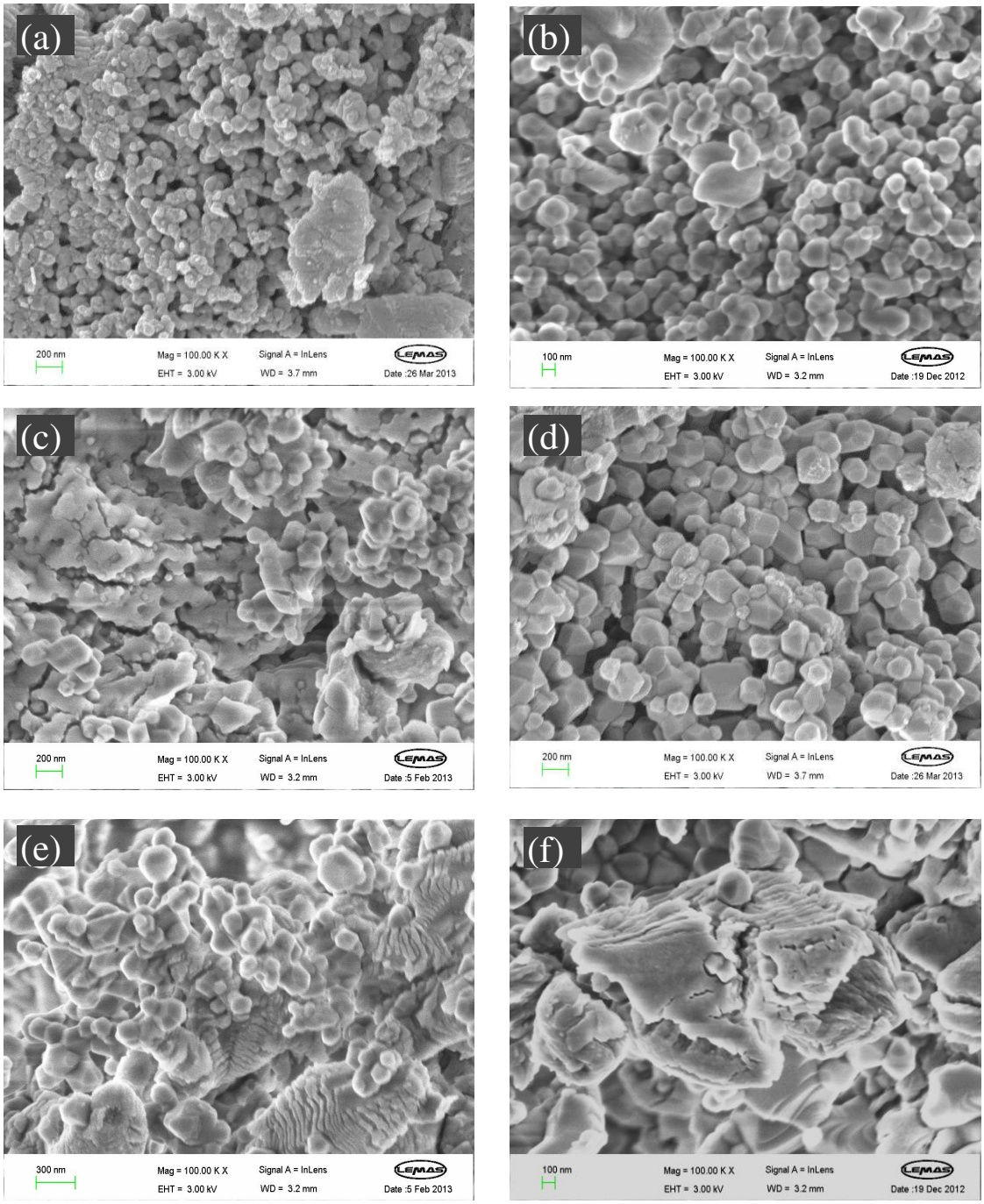

Fig. 3. SEM images of fresh and reacted catalysts showing the influence of catalytic reforming temperature (a) fresh 10 wt.% Ni-dolomite , (b) reacted 10 wt.% Ni-dolomite at 850 °C, (c) reacted at 900 °C, (d) reacted at 950 °C, (e) reacted at 1000 °C and (f) reacted at 1050 °C

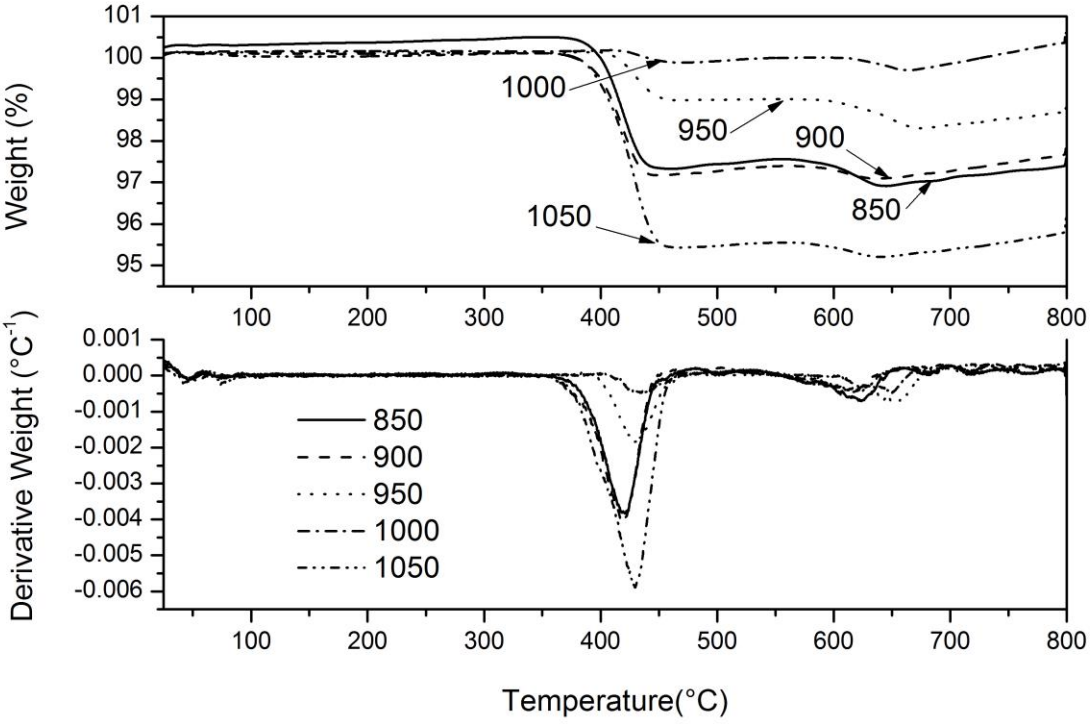

Fig. 4. TGA-TPO and DTG-TPO results showing the influence of catalytic reforming temperature on the amount of deposited carbon on reacted 10 wt.% Ni-dolomite catalyst

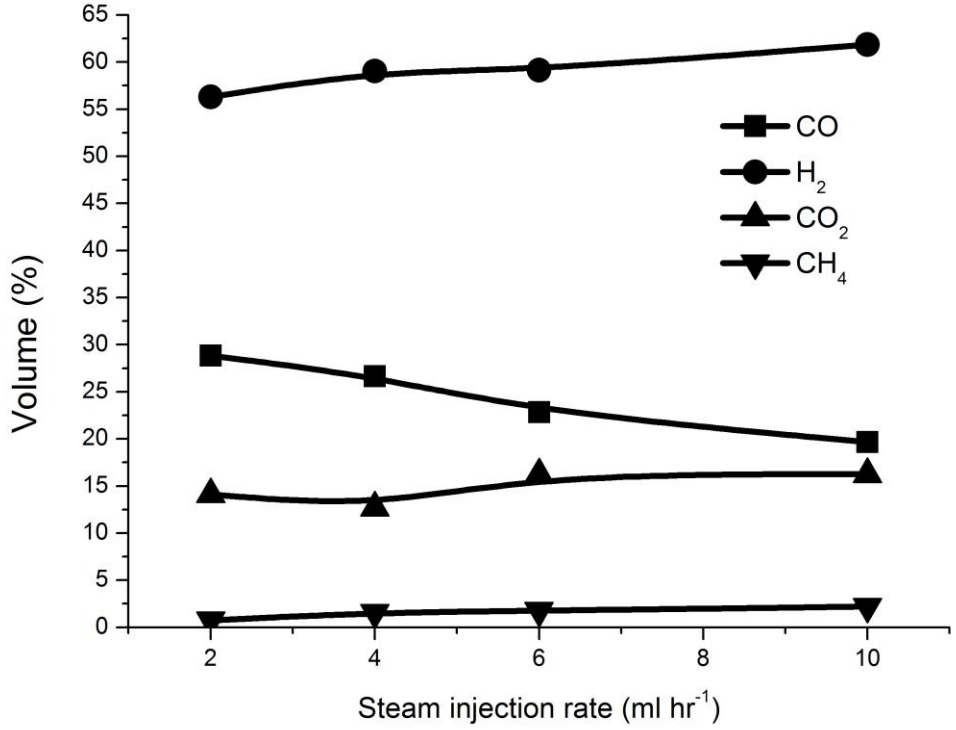

Fig. 5. The influence of steam flow rate on gas composition during the pyrolysis-catalytic reforming of rice husk (particle size 1.4 – 2.8 m.m. and catalyst temperature 950 °C).

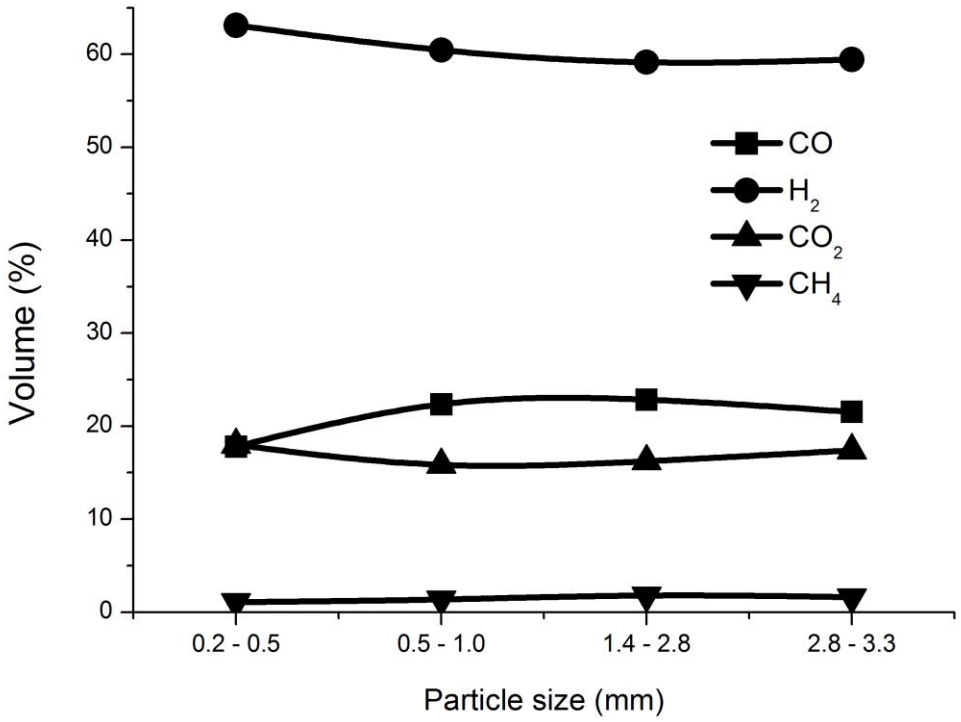

Fig. 6. The influence of particle size on gas composition during the pyrolysis-gasification of rice husk (catalyst temperature 950 °C and steam: biomass ratio 1.37).